UNSUPERVISED CURVATURE-BASED RETINAL VESSEL SEGMENTATION

Saurabh Garg, Jayanthi Sivaswamy, Siva Chandra

CVIT, International Institute of Information Technology, Hyderabad, India

ABSTRACT

Unsupervised methods for automatic vessel segmentation from retinal images are attractive when only small datasets, with associated ground truth markings, are available. We present an unsupervised, curvature-based method for segmenting the complete vessel tree from colour retinal images. The vessels are modeled as trenches and the medial lines of the trenches are extracted using the curvature information derived from a novel curvature estimate. The complete vessel structure is then extracted using a modified region growing method. Test-results of the algorithm using the DRIVE dataset are superior to previously reported unsupervised methods and comparable to those obtained with the supervised methods in [1],[2].

Index Terms— retina, curvature, vessel segmentation, unsupervised, ridge.

1. INTRODUCTION

Automatic segmentation of the vessel tree from colour retinal images has received much attention recently given its important role in image registration and in disease identification such as in diabetic retinopathy and hypertension. Techniques ranging from multi-level thresholding [3],[4] to model-based have been proposed. In the latter, information about the vessel morphology such as linearity, colouring, circular cross-section, etc., are used to construct feature sets which are used for either supervised classification or to devise filters for detection. Examples of unsupervised techniques include those based on matched filters [5],[6], morphological filters[7], and graph cuts [8], whereas examples of supervised techniques are ridge based [1] and wavelet based feature extraction [2].

Efforts to develop common datasets (with ground truth markings) for benchmarking various segmentation techniques are also slowly gaining pace [9],[4]. However, the size of these datasets is still small (maximum of 40) compared to the size of the datasets available for segmentation of non-medical images which are larger. A reason for this is the sensitive nature of the domain. Another factor is the need for involvement of medical experts in generating the ground truth, at least as guides, which may not be easy given other priorities for their time. Given this scenario, supervised approaches to segmentation result in reduction of the actual test set size as they require part of the available dataset to be used for training to tune parameters. Overall, such approaches can make it difficult to fully assess and benchmark different techniques and hinder the identification of robust techniques for deployment in mass screening programmes. Hence, we believe there is a critical need for taking an unsupervised approach to vessel segmentation that can perform as well as supervised approaches. We present one such solution for vessel segmetation from colour retinal images in this paper which performs well on a benchmark dataset.

We gratefully acknowledge DST, Govt. of India for funding.

2. PROPOSED ALGORITHM

When the green channel of a colour retinal image is visualised as a surface in 3D space, blood vessels form topographical trenches. Hence, the problem of blood vessel detection can be formulated as an image analysis problem of trench detection. Most techniques in literature use such a formulation to detect blood vessels, though the terminology commonly used is ridges, rather than trenches, by ignoring the sign of the curvature. These techniques are based on the fact that medial lines of trenches are characterised by high magnitudes of curvature along the direction perpendicular to the trench. Locating the medial lines of trenches generally requires detecting the points of directional maxima of the maximum principle curvature (MPC) [10] of the image surface. Calculation of MPC requires estimation of the first and second directional derivatives of the image function which is computationally complex and expensive. We propose a vessel detection technique based on an alternative curvature measure proposed in [11]. The first stage addresses the common problem of non-uniform illumination in retinal images due to both the retinal geometry and other imaging defects, while the second stage detects vessels via trench detection using curvature measurement. The output of this stage is in the form of a medial axes map of the vessels. The entire vessel structure is extracted next using a simple region growing technique. Each of these stages are described in detail next.

2.1. Illumination Correction

We address the non-uniform illumination problem by modifying a quotient based approach proposed for face images [12]. The non-uniform illumination in a given degraded retinal im-

age I, is modelled as a multiplicative degradation function L applied to an original image I_o. Assuming L to be a slowly varying function, it can be estimated by smoothing the degraded image. If I_s is the smoothed image then L can be found as:

$$L(x,y) = \begin{cases} \frac{I_s(x,y)}{l_o} & \text{if } I_s(x,y) < l_o \\ 1 & \text{if } I_s(x,y) \geq l_o. \end{cases}$$

where l_o is the desired mean illumination level, which can be chosen to be half the dynamic pixel range. Using the above estimate of the degradation, the desired corrected image is found as:

$$I_o(x,y) = \begin{cases} I(x,y) \times \frac{l_o}{I_s(x,y)} & \text{if } I_s(x,y) < l_o \\ I(x,y) & \text{if } I_s(x,y) \geq l_o. \end{cases}$$

2.2. Trench detection

Trenches are regions characterized by high curvature, oriented in a particular direction. The curvature at any point is a measure of the bend in the surface along a particular direction. In order to determine this curvature at every point in the image, we have chosen to use an alternative measure for curvature of an image surface that has been proposed in [11]. This is called the surface tangent derivative or the STD and its scope, as established in [11], indicates that it can be used to detect a wide range of trenches. We provide a brief summary of the STD next.

Let y = f(x) be any 1D function and the tangent at a point P on this function make an angle θ. The extrinsic curvature of the function f(x) at this point is given as:

$$\kappa(x) = \frac{d\theta}{dl} = \frac{\frac{d\theta}{dx}}{\sqrt{1 + \left(\frac{dy}{dx}\right)^2}} = \frac{\frac{d^2y}{dx^2}}{\left(1 + \left(\frac{dy}{dx}\right)^2\right)^{\frac{3}{2}}} \quad (1)$$

The numerator of the third term in the above expression, $\frac{d\theta}{dx}$, can be expanded as

$$\Upsilon(x) = \frac{d\theta}{dx} = \frac{d}{dx}\left[tan^{-1}\left(\frac{dy}{dx}\right)\right] = \frac{\frac{d^2y}{dx^2}}{1 + \left(\frac{dy}{dx}\right)^2} \quad (2)$$

Comparing the above equations, we see that the two expressions differ only in the power of the denominator. $\Upsilon(x)$ peaks at the points (same as $\kappa(x)$) where first derivative of the image function is zero and second derivative is a maximum. In the case of 2D images, $\Upsilon(x)$ corresponds to a derivative of the angle made by a surface tangent line with the image plane, in some direction and hence is the STD of the image function.

Given a digital image, the STD at every point in the image is obtained by finding the directional derivatives of its gradient direction in N directions. In practice, this is achieved in the following steps: Given an image $I(m,n)$ its gradient image $G_i(m,n)$ and the corresponding gradient angle $\theta_i(m,n)$ = $tan^{-1}(G_i)$ are computed for N directions; next, the STD $\Upsilon_i(x)$ is computed from the directional derivatives of θ. The medial points in the trenches are located by finding maximas (magnitude) of $\Upsilon_i(x)$ along some orientation. An algorithm for detecting these medial pixels is given below.

2.2.1. Trench detection algorithm

Let $I(n,m)$ be the image function. Calculate the STD $\Upsilon_i(n,m)$ for 4 directions with a mask of size $M \times M$. Let t be the threshold for trench strength. For every pixel location (n, m), do the following:
1. Evaluate $|\Upsilon_{max}|$ = max $\{ |\Upsilon_i| \}$ and let the corresponding orientation $i = \alpha$
2. If $|\Upsilon_{max}| > t$ then:
Check if $|\Upsilon_{max}| > |\Upsilon_i|$ of the neighboring pixels corresponding to the direction α. If yes, then mark the pixel (n,m) as a trench pixel. Else, do nothing.

The last test can be explained with an example. If $\alpha = 45^o$, then check if
$|\Upsilon_{max}| > |\Upsilon_i(n+1, m+1)|$ and
$|\Upsilon_{max}| > |\Upsilon_i(n-1, m-1)|$

The choice of the threshold t controls which part of the vessel tree is captured. For instance a high threshold will capture only the main branches which are relatively thick. As the threshold value is lowered, a fuller tree is captured along with many extraneous points which may not be part of the vessel tree. In order to address this problem, we have devised a solution based on the observation that thinner vessels branch out from thicker vessels. Thus, we initialise a trench map by setting a high threshold that captures the thickest branches. We reject isolated trench points in this map based on connectivity. Next, we lower the threshold and add newly detected trench pixels to the map based on their connectivity to those in the initial map. This scheme is described formally below.

2.2.2. Vessel reconstruction

Let Λ_h and Λ_l be the set of trench pixels obtained at threshold t_h and t_l respectively such that $t_h > t_l$. The reconstructed vessel map Λ_r is obtained as follows:
1. $\Lambda_r = \Lambda_h$
2. For every pixel $v \in \Lambda_l$, $\Lambda_r = \Lambda_r \cup v$, if v is 8-connected to at least one pixel in Λ_r
3. Repeat step 2 until no further pixel is added to Λ_r

2.3. Segmentation

A modified region growing scheme is used to segment the vessels. Since the region of interest is a vessel, domain knowledge can be exploited to constrain the growth of the region. Medial points detected by the trench detection algorithm serve as seed points. The region is grown only around a selected

Fig. 1. (a) Input colour image (b) Detected medial lines (c) Segmentated vessels

Table 1. Performance comparison of different methods

Method	A_z	**MAA**	D_c	**Comment**
Soares	0.952	-	0.137	Supervised
Staal	0.94	0.95	0.1358	Supervised
Our Method	0.9271	0.9361	0.1488	Unsupervised
Zana	0.875	0.94	0.2887	Unsupervised
Wenchao	0.85	-	0.1823	Unsupervised
Jiang	0.81	0.92	0.3268	Unsupervised

neighborhood of the seed point, whose size is determined based on the width of the largest vessel present in the image. The region is grown based on the connectivity of the test pixel with the previously declared vessel pixels and its intensity value. A final dilation step is applied to complete the vessel tree segmentation.

3. EXPERIMENTS AND RESULTS

The above algorithm for vessel segmentation was tested on the DRIVE dataset [9]. In our experiments, the desired mean illumination was chosen to be 120 and the STD was computated in four different directions: $0^o, 45^o, 90^o$ and 135^o using a mask size of 5×5. The threshold (t_h) value was chosen empirically to provide the best results. The DRIVE database contains 40 colour images divided into 20 training and 20 test images. The downloaded images were of size 565×584. Even though, the proposed algorithm is unsupervised, only the 20 test images were included in our testset similar to [7],[8]and [3], in order to benchmark against the reported methods. A test image with the detected medial lines of trenches and the extracted vessel tree are shown in Figure 1. In the literature, several performance measures have been reported for assessing vessel segmentation. These include area under the ROC (A_z), maximum average accuracy (MAA) and distance of ROC from the ideal point $(0, 1)$ in the ROC, denoted by D_c [13],[8]. The first measures the discriminative power of an algorithm with perfect score being 1. The MAA represents the proportion of the total number of correctly classified pixels (vessel and non-vessel) relative to the total number of pixels in the retinal region, which is a subregion bounded by a mask imposed by the imaging system. The last measure, D_c, represents the ability of an algorithm to maximise true positives without increasing the false positives in the detected results, with a lower value indicating better performance. We have used all these measures to compare our algorithm's performance against methods that have been reported in literature. A sample ground truth and segmented results are shown in Figure 2 for our algorithm and [1], [7] for comparison. These figures show that the vessel trees are of good quality with both the thick and thin vessels being successfuly extracted by our algorithm. Our algorithm is sensitive enough to consistently pick out even the finer vessels. Figure 3 shows the ROC for our algorithm along with those of the previously reported methods. The ROCs for the other methods have been duplicated from the respective papers for comparison. Table 1 shows a comparison of the A_z, MAA and D_c for the different supervised and unsupervised segmentation algorithms. It can be seen from the

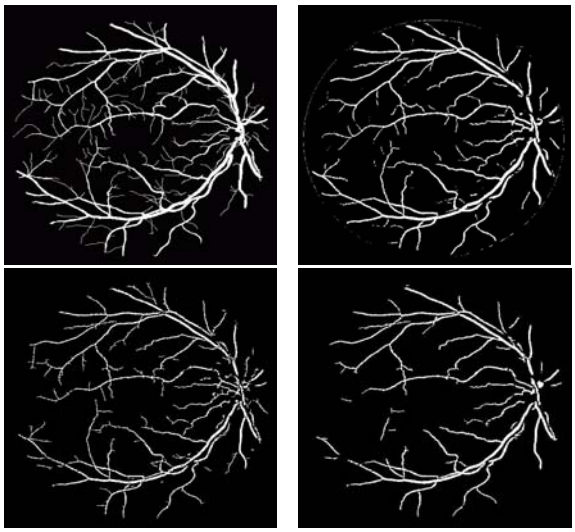

Fig. 2. Clockwise from top left (a) Ground truth (b) Staal results [1] (c) Zana results [7] (d) Our results

table that in general, supervised methods outperform unsupervised methods and our algorithm's performance is closer to the existing supervised methods. Specifically, in terms of discriminative power, our algorithm outperforms all other unsupervised methods and is closer to the supervised methods, while in terms of accuracy, the performance is comparable to the best unsupervised method reported in literature. The obtained result for D_c indicates that our novel curvature based approach is able to increase true positive rate without increasing the fasle positive rate unlike other unsupervised methods.

4. DISCUSSION AND CONCLUSION

Obtaining large datasets with ground truth is essential in developing robust solutions for vessel segmentation that can be used in mass programmes. However, this is difficult to achieve as the ground truth generation is a tedious process that demands patience. In the course of our experiments, we discovered that the ground truth markings in the DRIVE dataset tended to be oversegmented at times, perhaps as a sign of the above problem, in which case the vessel thickness obtained prior to the last dilation step in our algorithm was found to be closer to the true vessel thickness as detected by a Canny detector. This signals the challenges in creating consistent quality *and* large size datasets for testing and benchmarking segmentation algorithms. Unsupervised techniques for segmentation, such as the one we have presented, are hence quite attractive in this scenario. In registration applications, an added strength of our method is it can be simplified by removing the segmentation stage as the medial axis map provides sufficient corner (control) points.

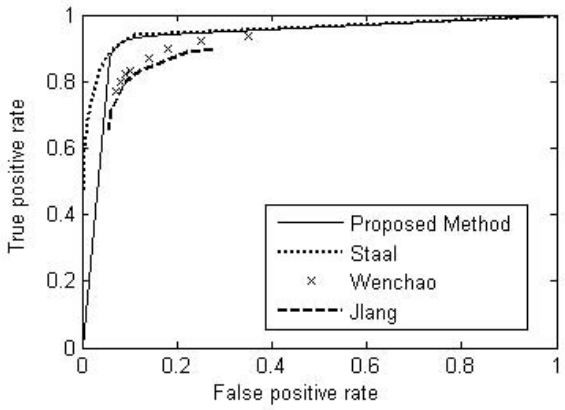

Fig. 3. Receiver Operator characteristics for different methods.

5. REFERENCES

[1] J. Staal, M. D. Abramoff, M. Niemeijer, M. A. Viergever, and B. Ginneken, "Ridge-based vessel segmentation in color images of retina," *IEEE Trans. Medical Imaging*, vol. 23(4), pp. 501–509, 2004.

[2] J. V. B. Soares, J. J. G. Leandro, R. M. Cesar-Jr., H. F. Jelinek, and M. J. Cree, "Retinal vessel segmentation using the 2-d gabor wavelet and supervised classification," *IEEE Trans. on Medical Imaging*, vol. 25, pp. 1214–1222, 2006.

[3] X. Jiang and D Mojon, "Adaptive local thresholding by verification-based multi-threshold probing with application to vessel detection in retinal images," *IEEE Trans. PAMI*, vol. 25(1), pp. 131–137, 2003.

[4] A. Hoover, V. Kouznetsova, and M. Goldbaum, "Locating blood vessels in retinal images by piecewise threshold probing of matched filter response," *IEEE Trans. Medical Imaging*, vol. 19(3), pp. 203–210, 2000.

[5] S. Chaudhuri and S. Chatterjee, "Detection of blood vessels in retinal images using two-dimensional matched filters," *IEEE Trans. Medical Imaging*, vol. 8(3), pp. 263–269, 1989.

[6] Thitiporn Chanwimaluang and Guoliang Fan, "An efficient blood vessel detection algorithm for retinal images, using entropy thresholding," *ISCAS*, vol. 5, pp. 21–24, 2003.

[7] F. Zana and J. Klein, "Segmentation of vessel-like patterns using mathematical morphology and curvature evaluation," *IEEE Trans. on Image Processing*, vol. 10(7), pp. 1010–1019, 2001.

[8] Wenchao Cai and Albert C.S. Chung, "Multi-resolution vessel segmentation using normalized cuts in retinal images," *MICCAI*, vol. LNCS 4191, pp. 928–936, 2006.

[9] "http://www.isi.uu.nl/research/databases/drive/," .

[10] D. Eberly, R. Gardner, B. Morse, S. Pizer, and C. Scharlach, "Ridges for image analysis," vol. 4, pp. 353–373, 1994.

[11] J.Sivaswamy, G.D.Joshi, and S. Chandra, "An alternative curvature measure for topographic feature detection," *To appear in Proc. Indian conference on vision, graphics and image processing*, 2006.

[12] Haitao Wang, Stan Z. Li, and Yangsheng Wang, "Generalized quotient image," *Proc. CVPR*, vol. 2, pp. 498–505, 2004.

[13] M. Niemeijer, J.J. Staal, B. van Ginneken, M. Loog, and M.D. Abramoff, "Comparative study of retinal vessel segmentation methods on a new publicly available database," *Proc. SPIE Conf. on Medical Imaging*, vol. 5370, pp. 648–656, 2004.